ELSEVIER

Brachytherapy 2 (2003) 207–214

BRACHYTHERAPY

Reduction of computed tomography metal artifacts due to the Fletcher-Suit applicator in gynecology patients receiving intracavitary brachytherapy

John C. Roeske[1,*], Christina Lund[1], Charles A. Pelizzari[1], Xiaochuan Pan[2], Arno J. Mundt[1]

[1]*Department of Radiation and Cellular Oncology, The University of Chicago, Chicago, IL*
[2]*Department of Radiology, The University of Chicago, Chicago, IL*

ABSTRACT

PURPOSE: To evaluate a method of reducing computed tomography (CT) metal artifacts due to the Fletcher-Suit applicator.

METHODS AND MATERIALS: We apply a projection-interpolation algorithm to CT images containing artifacts from the brachytherapy applicator. Regions of projection data containing the applicator are interpolated, removing the metal from the projections. A new image is then reconstructed, and a pixel-by-pixel correction factor applied to the original image to reduce the severity of metal artifacts. This technique is applied to phantom and patient image data.

RESULTS: Qualitative and quantitative comparisons of images produced before and after projection-interpolation show a significant reduction in metal artifacts. In patient images containing the tandem alone, this method almost completely eliminated the artifact. In slices containing both tandem and colpostats, the algorithm reduced artifacts but did not completely eliminate them.

CONCLUSIONS: The projection-interpolation method can be used to reduce the severity of metal artifacts caused by the Fletcher-Suit applicator.

Keywords: Brachytherapy; CT artifacts; Cervical cancer

Introduction

Cervical cancer is the third most common gynecologic malignancy in the United States occurring in approximately 15,000 women per year (1). Radiotherapy (RT) of these patients typically consists of a combination of whole pelvic RT (WPRT) and intracavitary brachytherapy (ICB). ICB is delivered at many institutions using low–dose-rate techniques with a Fletcher-Suit (FS) applicator that is afterloaded with ^{137}Cs sources. Following insertion of the applicator, treatment planning consists of first obtaining a set of orthogonal X-ray films, and then reconstructing individual source locations and normal tissue dose calculation points. Since soft tissue is not readily visible on diagnostic X-ray films, radiopaque packing, markers in the rectum or contrast in the Foley catheter bulb are used as surrogates. Dose is calculated to Point A, as well as bladder and rectal points. Source strengths are modified through an iterative process to maximize the difference between the Point A dose and the normal tissue dose points, while producing a "pear"-shaped dose distribution. The "pear" shape assures the delivery of tumorcidal doses to the primary tumor and parametrial tissues.

While this planning approach is commonplace, it has a number of limitations. Perhaps the most important limitation is that tumor geometry and normal structures are not incorporated into the planning process. Thus, the dose calculated to a limited number of points may not be representative of the dose delivered to the entire structure. Additionally, dose is prescribed relative to the cervical os (Point A) and may not encompass the distal portions of the tumor. Finally, treatment planning is a trial-and-error process that is both time consuming and may lead to a suboptimal plan.

Given these limitations, a number of investigators have explored the use of CT-based treatment planning (2–8). However, image artifacts produced by the metal applicator have limited the widespread adoption of CT-guided planning. A number of approaches have been used to minimize or

Received 3 April 2003; received in revised form 20 August 2003; accepted 22 August 2003.

* Corresponding author. Department of Radiation and Cellular Oncology, The University of Chicago, MC 9006 5758, S. Maryland Avenue, Chicago, IL 60637. Tel.: +1-773-702-6876; fax: +1-773-834-7299.

E-mail address: roeske@rover.bsd.uchicago.edu (J.C. Roeske).

1538-4721/03/$ – see front matter
doi:10.1016/j.brachy.2003.08.001

circumvent these artifacts (2–7). Post-processing techniques involve manipulating the image window and level to reduce the appearance of metal artifacts (2, 3, 7). Additionally, images can be reformatted into planes (other than the original axial) that are less sensitive to these artifacts. Complementary information (3, 7) such as orthogonal films or scout images from the CT scanner has also been used. Since neither of these images contain the metal artifacts, the source locations can be readily determined, and used in conjunction with CT images (containing the artifacts) to display the 3-D dose distribution. Others have considered the use of CT-compatible applicators (4–6, 8) that are constructed of titanium or plastic.

An alternative approach involves attempting to reduce the artifacts at the time of image reconstruction by minimizing the inconsistency in the projection data caused by the high density metal. The projection-interpolation (9–11) method artificially generates the missing or incomplete data within individual CT projections using linear (or higher order) interpolation. This approach has been used for hip prostheses (11), surgical clips (10) and other smaller metal objects within the body. However, to our knowledge, it has not been applied to ICB. The goal of this work is to apply the projection-interpolation algorithm to images containing the ICB applicator in order to evaluate its effectiveness in reducing the magnitude of CT metal artifacts. Results will be presented for both phantom and patient images obtained with our departmental scanner.

Methods and materials

Reconstruction of CT images

CT image reconstruction is a two-step process. Initially, the patient is placed in the scanner while an X-ray beam rotates about a fixed point. As the beam sweeps around the patient, detectors measure the pattern of radiation (projection) transmitted through the patient. Next, image reconstruction from these projections is performed through a process known as filtered backprojection (FBP). Metal artifacts arise because the attenuation coefficient for diagnostic X-rays in metal is much higher than in soft tissue and bone. Thus, each CT projection of the object contains a region, in the shadow of the metal object, where virtually no radiation is detected. A region of zero radiation in a projection violates one of the basic assumptions of standard CT reconstruction algorithms. Attempting to reconstruct such data using filtered backprojection (FBP) leads to artifacts reflecting the inconsistency of the projection data.

Projection-interpolation algorithm

The goal of the projection-interpolation technique is to reduce the artifacts caused by missing or incomplete projection data by interpolating through the projection of the applicator. The algorithm is implemented as follows. Initially, a CT scan of the phantom or patient, containing the metal object, is obtained. An axial image (image 1) is reconstructed from the original projection data using a standard FBP technique (12). This image has the artifacts present; however, the edges of the reconstructed applicator can be well visualized by appropriate window and leveling. The next step involves segmenting the object and eliminating the surrounding image. A new image (image 2) is thus created that consists only of the segmented applicator. At each angle, these data are re-projected and used to determine the regions of inconsistency in the original projections over which interpolation needs to be applied. The original projection dataset is interpolated across these regions using a cubic spline fit. A schematic diagram is shown in Fig. 1. The peak represents the projection of the metallic object at a given angle. The vertical lines are the projected edges of the object as determined from image 2. Interpolation is performed between the two lines to eliminate the object from the projection. This process is repeated until interpolation is performed on all image projections.

An example of this interpolation for all image projections is shown in Figs. 2a and 2b. These images are sinograms where each row in the image represents a different projection angle. The region corresponding to the metal object, shown as the bright feature near the center of the image (Fig. 2a), is removed and interpolated over all projections to produce Fig. 2b. These interpolated projections are then used to reconstruct a new image (image 3) in which both the artifacts and metal object are removed. A correction factor is applied on a pixel-by-pixel basis to image 1 to create the artifact-reduced image. This correction factor is given by:

$$C(x,y) = \text{image } 3(x,y)/\text{image } 1(x,y) \text{ for } x,y \text{ in the artifact region } 1$$
$$C(x,y) = 1 \text{ for all other regions.}$$

A program was written to implement the above algorithm using the Interactive Data Language (IDL; RSI, Boulder, CO). The program reads the projection data from the CT scanner, constructs an axial image and allows the user to adjust the window and level in order to highlight the approximate region of the applicator. Next, the program re-projects the segmented object and applies the interpolation scheme to the sinogram. The time for image reconstruction, re-projection and correction is approximately 5–10 s per image on a desktop personal computer.

Phantom data

A phantom was constructed to evaluate the ability of this algorithm to reduce metal artifacts. This phantom consisted of a Fletcher-Suit applicator embedded in a block of masonite. Additionally, a metal disk was inserted to represent a high contrast object in the region—such as contrast in the Foley bulb. The phantom was scanned in the axial mode with a 3-mm slice thickness and table index on a PQ5000 CT

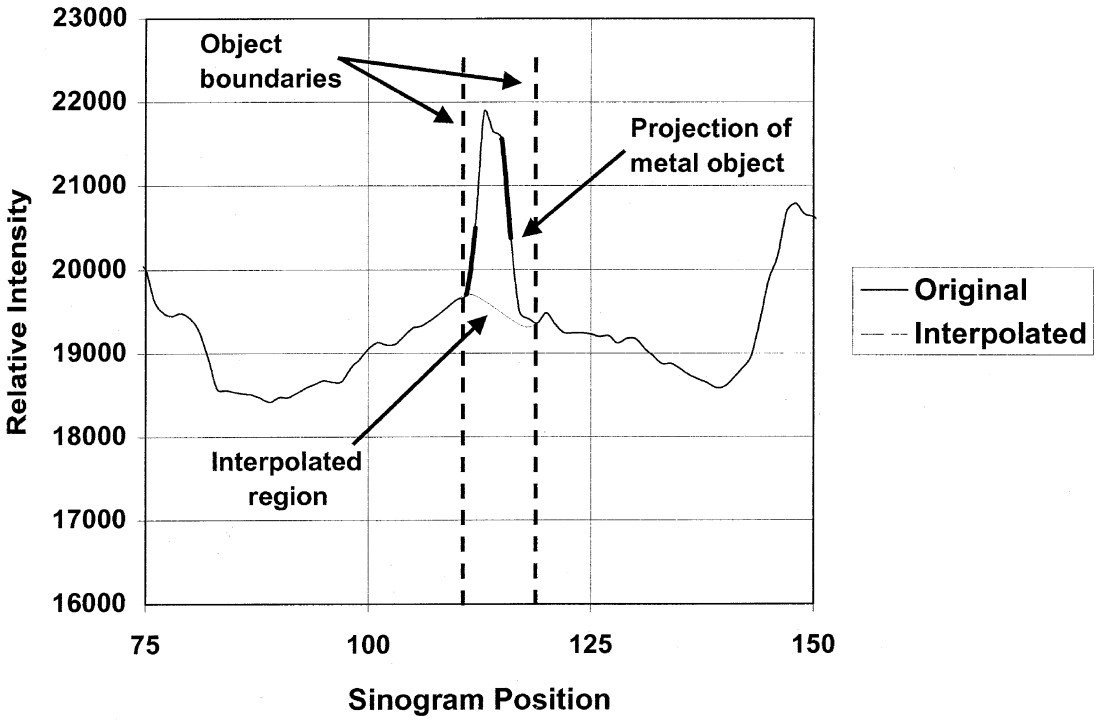

Fig. 1. A CT projection through a metal artifact. The interpolation algorithm identifies the boundary of the applicator and performs cubic spline interpolation through the applicator. The applicator signal is suppressed and a consistent data set is formed.

scanner (Marconi, Cleveland, OH). Projection data were saved during acquisition for reconstruction of the phantom. The raw data consisted of projections at 1200 gantry positions with each projection composed of 1024 pixels. Since these projections were obtained in a fan beam geometry, they were converted to a parallel beam geometry (for ease of computation) using the method described by Pan (13). These images were then reconstructed using FBP and the algorithm described previously.

Patient data

Similarly, a patient was scanned in whom the Fletcher-Suit applicator was inserted. This patient had early stage

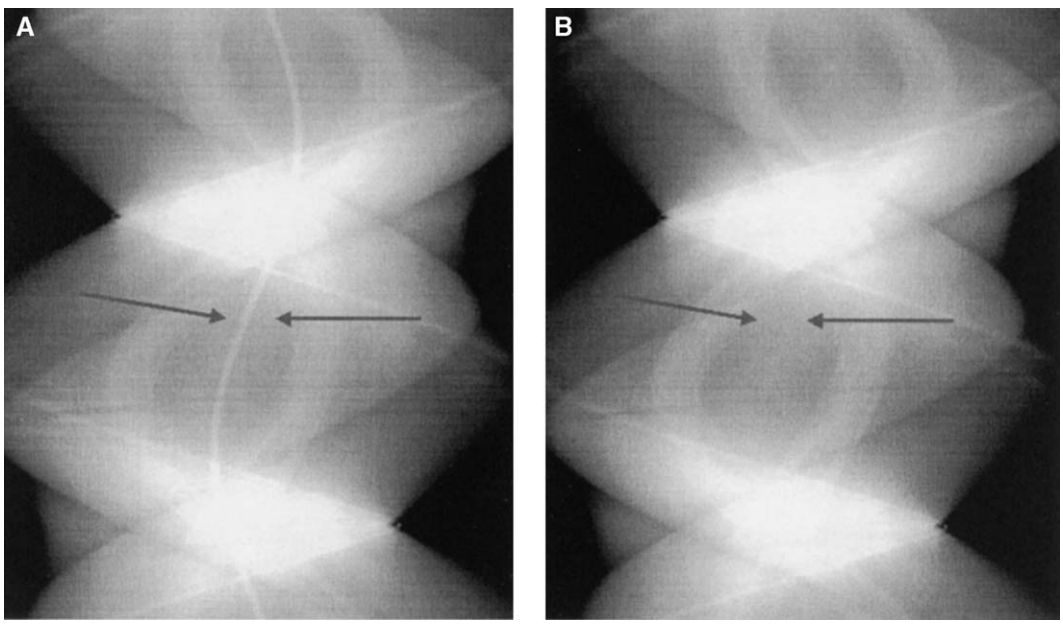

Fig. 2. Sinogram of the image data for the phantom. (a) Raw sinogram. The high intensity areas (between the arrows) represent the metal. (b) An example of the sinogram after interpolation. Note that the metal is no longer present.

cervical cancer and received 45 Gy WPRT. ICB was used to deliver an additional 40 Gy to Point A (85 Gy total). The patient was scanned from the top of the tandem to below the colpostats with a 3 mm slice thickness and table index. Raw projection data were saved and subsequently reconstructed using the above algorithm.

Results

The results for the phantom experiment are shown in Figs. 3a and 3b. In this simple case, two metal objects are located near the center of the phantom. In a patient, these objects would be representative of the contrast in the Foley bulb and the tandem. The artifacts introduced by the metal include a streaking observed emanating from the upper object, and a low density (dark) region located between the two objects (Fig. 3a). The image reconstructed using the projection-interpolation algorithm is shown in Fig. 3b. Note that the high-density streaks are no longer evident, and the region of reduced density between the objects nearly blends in with the surrounding region. A vertical profile through the two metal objects is shown in Fig. 4. Plotted on the y-axis is the relative CT pixel value as a function of position (x-axis). Regions that appeared lower in density on the original CT image (between the metal objects) now have a relative CT value that is similar to the remainder of the phantom.

Three representative slices of the patient scanned with the FS applicator in place are shown in Figs. 5–7. These images consist of reconstructions through the tandem alone (Figs. 5a and 5b), through the upper portion of the colpostats, tandem, and Foley bulb (Figs. 6a and 6b), and through the center of the colpostats, tandem, and Foley bulb (Figs. 7a and 7b). In each case, the left figure represents the uncorrected image and the right figure represents the corrected image. The uncorrected image of the tandem alone (Fig. 5a) shows only minor streaking artifacts. As seen in the phantom example, application of the projection-interpolation algorithm (Fig. 5b), almost completely eliminates these metal artifacts.

The second image set (Figs. 6a and 6b) is through the top of the colpostats and shows the contrast in the Foley catheter as well. Because of the many high-density metal objects, the resultant artifacts are more pronounced than on the previous slice. Application of the projection-interpolation algorithm shows that the streaking regions, as well as the low-density regions are reduced. However, the algorithm did not perform as well as on the previous slice. Due to the inclusion of four high-density objects (bladder contrast, tandem, and two colpostats), a relatively larger portion of each projection must be interpolated. The net result is that interpolation may not be as representative of the underlying densities, and therefore may introduce additional artifacts.

Finally, a CT slice through the center of the colpostats is shown in Figs. 7a and 7b. This uncorrected image shows a high degree of streaking artifacts due to the presence of the tungsten shielding in the colpostats. The corrected image reconstructed using projection-interpolation shows that the artifacts are reduced significantly. However, again, a relatively large region of the projection data is interpolated. Hence, the algorithm reduces the magnitude of the artifacts, but does not completely eliminate them.

Discussion

We have described here a method to reduce the magnitude of CT artifacts due to a conventional Fletcher-Suit applicator.

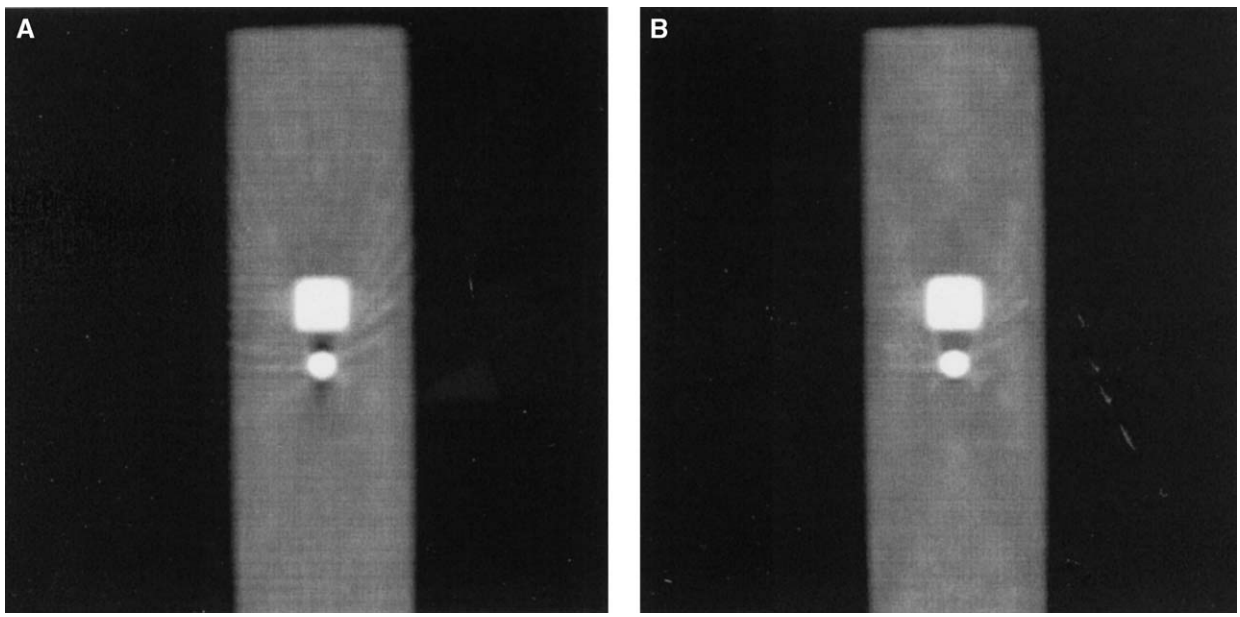

Fig. 3. CT reconstruction of a phantom. (a) Image of the phantom reconstructed using a standard FBP algorithm. (b) Artifact-reduced image.

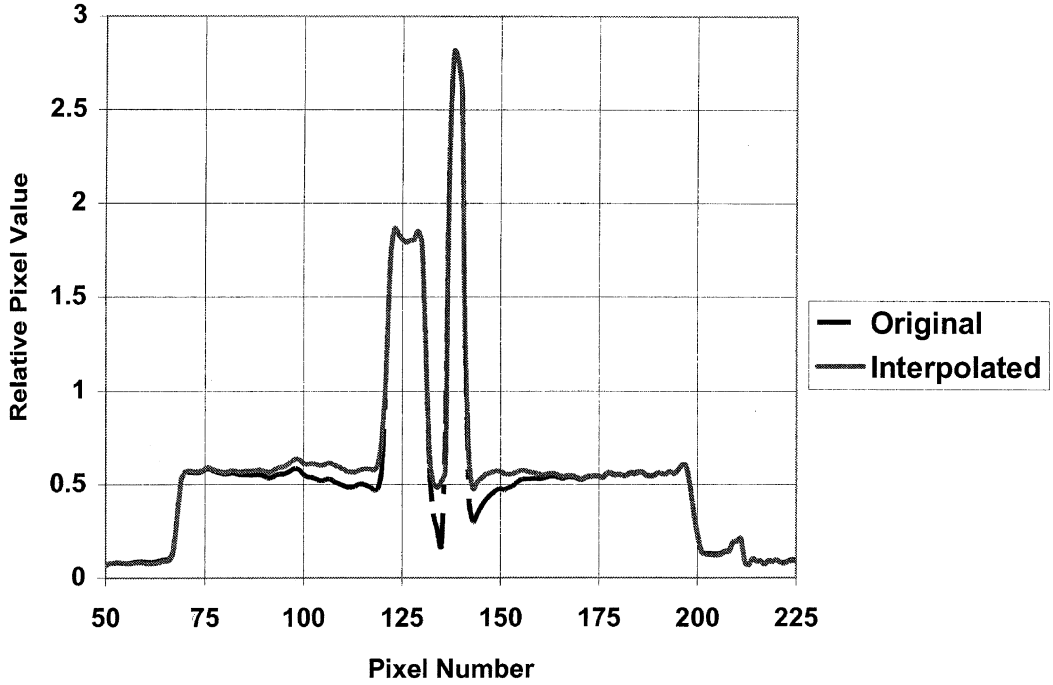

Fig. 4. A scan of pixel values through the phantom showing a comparison of the relative pixel value both before and after artifact reduction.

This technique uses a projection-interpolation scheme to fill in areas of the projection data that include the applicator or other high-density materials. The interpolated projections are then reconstructed using FBP to form an image with both the applicator and artifact removed. By applying an appropriate correction factor to those pixels that form the artifacts, an artifact-reduced version of the original image is created. Our results indicate that in images containing one or two small objects, such as the tandem and catheter bulb, the algorithm performs well. However, in images containing three or four objects, interpolation is performed over a larger region of the projection data. Thus, the interpolation becomes less reliable and the artifacts are not completely removed. Nevertheless, the magnitude of these artifacts appears greatly reduced. In addition, the projection-interpolation algorithm may distort the tissues directly around the

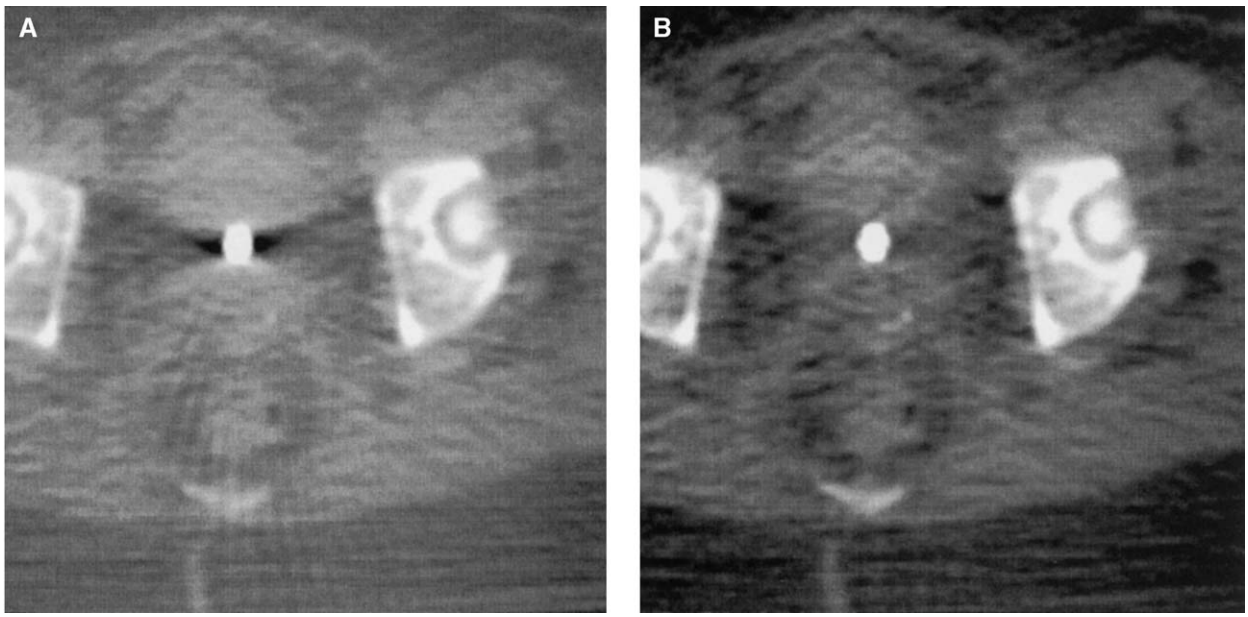

Fig. 5. CT scan through the tandem of a Fletcher-Suit applicator (a) before and (b) after artifact reduction.

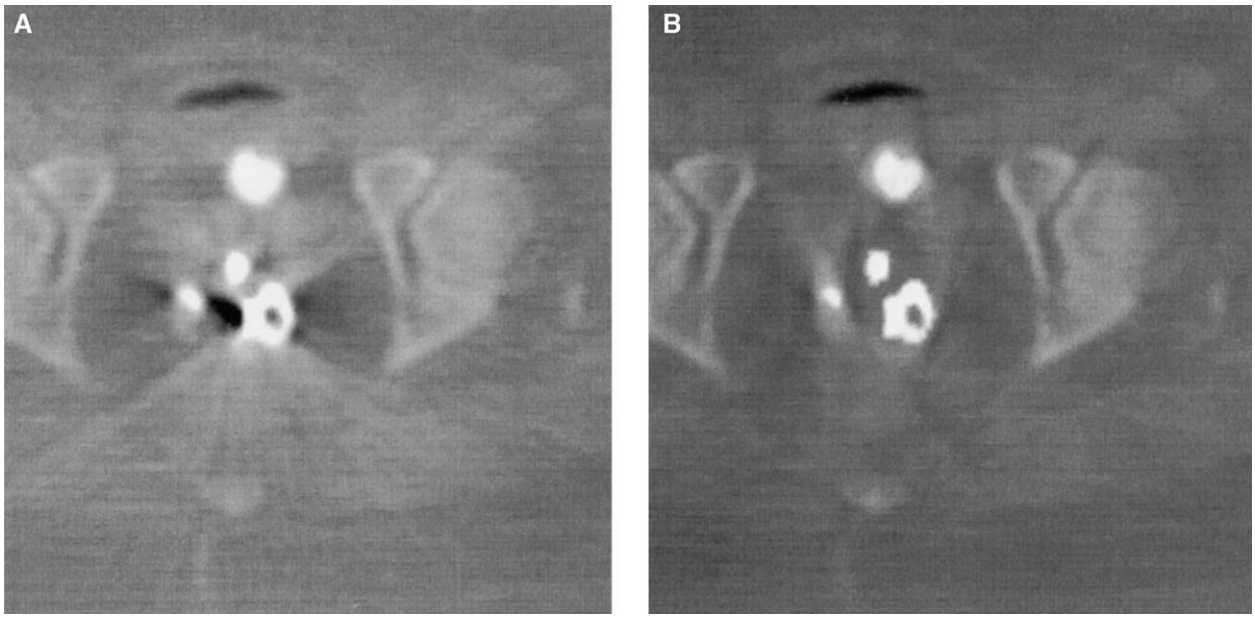

Fig. 6. CT scan showing the top of the colpostats, tandem and contrast in the Foley catheter (a) before and (b) after artifact reduction.

applicator due to misrepresentation of the underlying tissue densities caused by reconstruction of interpolated projections. However, such distortions are not expected to impede CT-based brachytherapy planning.

The principal advantage of this technique is the ease of use and short computational time. There is relatively little user interaction other than identifying the approximate edges of the applicator and the artifact region to be corrected. Additionally, full image reconstruction and artifact reduction can be performed in 5–10 s on a standard personal computer making the technique clinically useful. Since ICB treatment planning is often performed while the patient is waiting, methods that do not add significant time to the planning process are highly desirable.

Other techniques that use iterative reconstruction methods may further reduce the magnitude of metal artifacts. One such technique is known as iterative deblurring (14, 15). Briefly, this algorithm makes an initial "guess" of the image (such as an image with a uniform pixel value). Projections are then obtained of this "guess" image and compared to

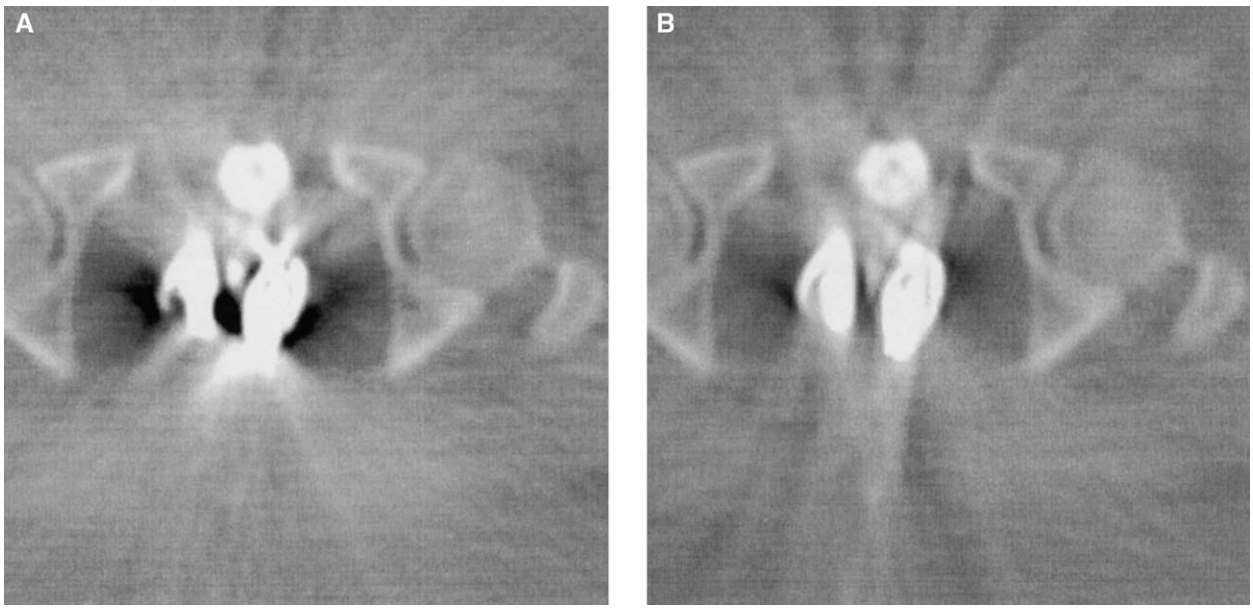

Fig. 7. CT slice through the center of the colpostats (a) before and (b) after artifact reduction.

the measured projections. By reconstructing the ratio of the measured to "guess" projections, an improved estimate of the image is obtained. This process can be repeated to minimize the difference between the measured and "guess" projections. The algorithm places an additional constraint such that regions in the sinogram and pixels in the reconstructed image containing the metal are ignored. Thus, an image with the absence of the artifact can be produced. While iterative techniques offer the potential for an improved image over the projection-interpolation approach, particularly in regions containing multiple objects, the technique is computationally intensive requiring 80–100 iterations per image (14). An alternative approach may be to use the iterative algorithm over a limited portion of the image. In a recent study by Xia *et al*. (16), an iterative algorithm was used to reconstruct only the metal portion of the image, while the projection-interpolation algorithm was used to reconstruct the surrounding tissues. In both simulation and patient studies, this approach resulted in significant artifact reduction with only minor increases in computational time (relative to the projection-interpolation algorithm).

Using the corrected images obtained from the projection-interpolation method, CT-based ICB treatment planning should be feasible. CT-based planning has been performed by others (2–8) who observed a significant variation in the maximum doses to normal tissues compared to conventional planning. Ling *et al.* (3) applied CT-based planning to 8 patients who received gynecological implants with the standard FS applicator. Through window and leveling of the CT image, they were able to delineate the bladder and rectal boundaries to be used in conjunction with 3-D dose calculations. Their results indicated that the maximum dose to the bladder was on average a factor of two larger with CT-based planning compared to doses obtained using orthogonal films. Similar results were observed for the maximum rectal doses. Schoeppel *et al.* (6) used a CT-compatible applicator to compare the dosimetry of 10 patients using both conventional and 3-D treatment planning methods. The ratio of the maximum bladder dose obtained using 3-D methods to the conventional approach was on average 2.1. For the rectum, the average value of this ratio was 1.6. Additionally, they observed a minimum dose to the cervix that was much lower than the Point A dose. In each of these studies the conclusions are the same—there is significant variation in the doses received by the bladder and rectum, and the doses calculated using the conventional method generally underestimated the doses calculated using CT-guided methods.

The realization of CT-based planning may also allow for more sophisticated treatment planning. For example, it would be desirable to use the 3-D information to take into account applicator shielding (17, 18). Furthermore, it would be useful to combine the 3-D brachytherapy dose distributions with a 3-D WPRT plan. At our institution, we are considering methods to combine intensity-modulated WPRT (IM-WPRT) dose distributions with brachytherapy planning (19–21). However, combining these dose distributions is not simple. First, since the patient may not be in the same position at the time of each planning scan, a global transformation is required to align the IM-WPRT and ICB planning images. Next, due to the presence of the applicator, the normal tissues in the ICB images will be distorted relative to the IM-WPRT images. Hence, a method of image warping would need to be applied in order to map the dose distribution from the IM-WPRT image set into the ICB set. Finally, optimization of the ICB plan could be performed taking into account the dose delivered by the IM-WPRT plan. Such an approach is years away, but offers the potential of improving local control while reducing chronic radiation sequelae in these patients.

Acknowledgments

This work is supported by a grant from the Whitaker Foundation.

References

[1] Parker SL, Tong T, Wingo PA. Cancer Statistics, 1996. *Cancer J Clin* 1996;65:5–27.
[2] Sewchand W, Prempree T, Patanaphan V, *et al*. Value of multi-planar CT images in interactive dosimetry planning of intracavitary therapy. *Int J Radiat Oncol Biol Phys* 1982;8:295–301.
[3] Ling CC, Schell MC, Working KR, *et al*. CT-assisted assessment of bladder and rectum dose in gynecological implants. *Int J Radiat Oncol Biol Phys* 1987;13:1577–1582.
[4] Schoeppel SL, Fraass BA, Hopkins MP, *et al*. A CT-compatible version of the Fletcher system intracavitary applicator: Clinical application and 3-dimensional treatment planning. *Int J Radiat Oncol Biol Phys* 1989;17:1103–1109.
[5] Weeks SJ, Dennett JC. Dose calculation and measurements for a CT-compatible version of the Fletcher applicator. *Int J Radiat Oncol Biol Phys* 1990;18:1191–1198.
[6] Schoeppel SL, LaVigne ML, Martel MK, *et al*. Three-dimensional treatment planning of intracavitary gynecologic implants: Analysis of ten cases and implications for dose specification. *Int J Radiat Oncol Biol Phys* 1994;28:277–283.
[7] Li S. Computer-aided gynecologic intracavitary brachytherapy [Ph.D. dissertation]. Chicago, IL: The University of Chicago; 1995.
[8] Weeks KJ, Montana GS. Three-dimensional applicator system for carcinoma of the uterine cervix. *Int J Radiat Oncol Biol Phys* 1997;37: 455–463.
[9] Lewitt RM, Bates RHT. Image reconstruction from projections: Projection completion methods. *Optik* 1978;50:189–204.
[10] Glover GH, Pelc NJ. An algorithm for the reduction of metal clip artifacts in CT reconstructions. *Med Phys* 1981;8:799–807.
[11] Kalendar WA, Hegel R, Ebersberger J. Reduction of CT artifacts caused by metallic implants. *Radiology* 1987;164:576–577.
[12] Brooks RA, DiChiro G. Theory of image reconstruction in computed tomography. *Radiology* 1975;117:561–572.
[13] Pan X. Optimal noise control in and fast reconstruction for a fan-beam computed tomography image. *Med Phys* 1999;26:689–697.
[14] Wang G, Snyder DJ, O'Sullivan JA, *et al*. Iterative deblurring for CT metal artifact reduction. *IEEE Trans Med Imag* 1996;15:657–664.
[15] Robertson DD, Yuan J, Wang G, *et al*. Total hip prosthesis metal-artifact suppression using iterative deblurring reconstruction. *J Comput Assist Tomogr* 1997;21:293–298.

[16] Xia D, Yu L, Pan X, et al. Comparative studies on algorithms for metal artifact reduction in CT image reconstruction. Presented at the 45th Annual Meeting of the American Association of Physicists in Medicine, San Diego, California, August 2003.

[17] Williamson JF. Dose calculations about shielded gynecological colpostats. *Int J Radiat Oncol Biol Phys* 1990;19:167–178.

[18] Gebara WJ, Weeks KJ, Hahn CA, *et al*. Computer assisted tomography tandem and ovoids (CATTO): A 3D CT-based assessment of bladder and rectal doses. *Rad Onc Invest* 1998;6:268–275.

[19] Roeske JC, Lujan A, Rotmensch J, *et al*. Intensity modulated whole pelvic radiation therapy in patients with gynecological malignancies. *Int J Radiat Oncol Biol Phys* 2000;48:1613–1621.

[20] Mundt AJ, Roeske JC, Lujan A, *et al*. Initial clinical experience using intensity modulated whole pelvic radiation therapy for gynecologic malignancies. *Gynecol Oncol* 2001;82:456–463.

[21] Mundt AJ, Lujan AE, Rotmensch J, *et al*. Intensity modulated whole pelvic radiation therapy in women with gynecologic malignancies. *Int J Radiat Oncol Biol Phys* 2002;52:1330–1337.